MNRAS 000, 1–11 (2017) Preprint 7 March 2024 Compiled using MNRAS LATEX style file v3.0

Jet quenching in the neutron star low-mass X-ray binary 1RXS J180408.9−342058

N.V. Gusinskaia,[1⋆] A.T. Deller,[2,5] J.W.T. Hessels,[1,2] N. Degenaar,[1,3]
J.C.A. Miller-Jones,[4] R. Wijnands,[1] A.S. Parikh,[1] T.D. Russell,[1] D. Altamirano[6]
[1]*Anton Pannekoek Institute for Astronomy, University of Amsterdam, Science Park 904, 1098 XH Amsterdam, The Netherlands*
[2]*ASTRON, the Netherlands Institute for Radio Astronomy, Postbus 2, 7990 AA, Dwingeloo, The Netherlands*
[3]*Institute of Astronomy, University of Cambridge, Madingley Road, Cambridge, CB3 OHA, UK*
[4]*International Centre for Radio Astronomy Research, Curtin University. GPO Box U1987, Perth, WA 6845, Australia*
[5]*Centre for Astrophysics and Supercomputing, Swinburne University of Technology, P.O. Box 218, Hawthorn, VIC 3122, Australia*
[6]*Department of Physics and Astronomy, University of Southampton, Southampton, Hampshire SO17 1BJ, UK*

arXiv:1705.06795v1 [astro-ph.HE] 18 May 2017

Accepted xxxx xxx xx. Received xxx xxxx xx; in original form 2017 April 12

ABSTRACT

We present quasi-simultaneous radio (VLA) and X-ray (*Swift*) observations of the neutron star low-mass X-ray binary (NS-LMXB) 1RXS J180408.9−342058 (J1804) during its 2015 outburst. We found that the radio jet of J1804 was bright ($232 \pm 4\,\mu$Jy at 10 GHz) during the initial hard X-ray state, before being quenched by more than an order of magnitude during the soft X-ray state ($19 \pm 4\,\mu$Jy). The source then was undetected in radio ($< 13\ \mu$Jy) as it faded to quiescence. In NS-LMXBs, possible jet quenching has been observed in only three sources and the J1804 jet quenching we show here is the deepest and clearest example to date. Radio observations when the source was fading towards quiescence ($L_X = 10^{34-35}\,\mathrm{erg\,s^{-1}}$) show that J1804 must follow a steep track in the radio/X-ray luminosity plane with $\beta > 0.7$ (where $L_R \propto L_X^{\beta}$). Few other sources have been studied in this faint regime, but a steep track is inconsistent with the suggested behaviour for the recently identified class of transitional millisecond pulsars. J1804 also shows fainter radio emission at $L_X < 10^{35}\,\mathrm{erg\,s^{-1}}$ than what is typically observed for accreting millisecond pulsars. This suggests that J1804 is likely not an accreting X-ray or transitional millisecond pulsar.

Key words:
Low mass X-ray binary – Radio/X-ray correlation – Disk/jet coupling – Sources, individual: 1RXS J180408.9−342058

1 INTRODUCTION

Accretion is a fundamental astrophysical process that occurs in a very broad range of astrophysical contexts, e.g. from proto-stars and planetary systems, to stellar-mass compact objects in short-orbit binaries, to active galactic nuclei (AGNe). Low-mass X-ray binaries (LMXBs) are binary systems with a neutron star (NS) or stellar-mass black hole (BH) primary and a low-mass ($< 1\,\mathrm{M}_\odot$) secondary star (which may be semi-degenerate or not). Most of the time, LMXBs are in a so-called quiescent state (where the X-ray luminosity, L_X, is $< 10^{34}$ erg/s). Many of these systems undergo episodic outbursts, where the accretion rate increases by orders of magnitude, and the system exhibits enhanced radiation. During outburst, emission is typically the strongest in the X-ray band (usually associated with the accretion inflow, disk and corona; Shakura & Sunyaev 1973, Begelman et al. 1983) and radio emission is often observed, indicative of a jet or another type of outflow (Fender et al. 2004a). LMXB outbursts have time scales of weeks to years, allowing us to investigate accretion in detail and in a dynamic way. LMXBs with black hole primaries (BH-LMXBs) are radio brighter at a given L_X and are to date arguably better characterized in the radio in comparison to NS-LMXBs (Fender & Kuulkers 2001; Migliari & Fender 2006).

A typical BH-LMXB outburst starts in a hard X-ray spectral state, where the X-ray spectrum is dominated by a hard power law component (see McClintock & Remillard 2006 and references therein). In some models, this state is characterised by a truncated accretion disk, where soft X-ray photons from the disk are Comptonized in an electron corona

⋆ E-mail: N.Gusinskaia@uva.nl

© 2017 The Authors

around the compact object (see e.g. Esin et al. 1997). In this state, radio emission is often detected and is associated with optically thick synchrotron radiation from a steady, self-absorbed, compact jet (e.g. Fender et al. 2004b, Fender et al. 2009). As the outburst progresses, the disk brightens due to an increased mass accretion rate. As the X-ray luminosity increases, the inner accretion disk moves inwards, closer to the central object (see e.g. Malzac 2007). The X-ray emission becomes dominated by a soft thermal component (described by blackbody emission from the hot inner region of the accretion disk), as the system moves towards the soft X-ray state. During this transition the brightest radio emission is observed. This emission is associated with optically-thin radio ejecta moving away from the system, which have been spatially resolved in a few BH-LMXBs (e.g. Mirabel & Rodríguez 1994). At this time, the steady jet is quenched (Russell et al. 2011; Corbel et al. 2004), appearing again in the reverse transition back to the hard state. At the peak of the outburst, BH-LMXBs can make several transitions between the hard and soft states (Fender et al. 2004b).

NS-LMXBs often exhibit hard and soft X-ray states similar those seen in BH-LMXBs. Historically, there are two classes of NS-LMXBs, defined by their shape in an X-ray color-color diagram: Z-type and Atoll-type NS-LMXBs (Hasinger & van der Klis 1989). Z-type sources accrete at higher accretion rates and generally have softer spectra than Atoll-type NSs. However, some transient sources have exhibited both Atoll and Z-type behaviour at low and high accretion rates, respectively (e.g. Homan et al. 2010; Homan et al. 2014). This indicates that these two types of behaviour are driven by a changing mass accretion rate and not a fundamental difference in source type.

Two other subclasses of NS-LMXBs are accreting millisecond X-ray pulsars (AMXPs) and transitional millisecond pulsars (tMSPs). During their outburst phases, AMXPs exhibit coherent X-ray pulsations as a result of the accretion flow being channeled by the NS's magnetic field onto its polar caps (Patruno & Watts 2012). tMSPs are NSs that switch between rotation-powered radio pulsar and accretion-powered LMXB phases (currently, only three confirmed transitional sources are known; see Bogdanov et al. 2015). Similar to Atoll and Z-type NSs, AMXPs and tMSPs could also be different manifestations of the same source class, as implied by M28I exhibiting both AMXP and tMSP behaviour at different mass accretion rates (Papitto et al. 2013).

Simultaneously observing LMXBs in the X-ray and radio bands allows us to explore connections between the inflow and outflow of material, investigating the relationship between radio brightness and the X-ray spectral state. Comparing the radio/X-ray correlation for different classes of accreting binaries allows us to investigate the influence of physical characteristics such as mass of the accretor, absence or presence of a stellar surface, and the strength of the magnetic field, on jet launching.

For BH-LMXBs there is a correlation between the radio (L_R) and X-ray (L_X) luminosities in the hard X-ray state, when the radio jet is steady, all the way down to quiescence (Corbel et al. 2000; Gallo et al. 2003; Gallo et al. 2006; Gallo et al. 2014). This relation is described by a powerlaw, such that $L_R \propto L_X^{\beta}$, where $\beta \sim 0.63$, which holds over more than eight orders of magnitude in X-ray luminosity and ∼four-five orders of magnitude in radio luminosity (see Gallo et al. 2003 and black circles in Fig. 1). This correlation can be expanded to encompass supermassive BHs and AGNe by using a mass scaling (the so-called 'fundamental plane of BH activity'; for more details see Merloni et al. 2003; Falcke et al. 2004; Plotkin et al. 2012). This power-law index is thought to be due to either accretion onto a BH being radiatively inefficient because infalling matter and energy is able to pass beyond the event horizon (Narayan & Yi 1995), or because BHs channel a significant fraction of the accretion energy into the jets (Fender et al. 2003). However, there are also 'radio-quiet outliers' (e.g. H1743−322, Figure 1; Coriat et al. 2011) which show a steeper correlation, where $\beta \approx 1 - 1.4$ at higher X-ray luminosities ($L_X \geq 10^{36}$ erg/s; Gallo et al. 2012), implying radiatively-efficient accretion (see Figure 1). At lower X-ray luminosities these objects appear to rejoin the 'standard' radiatively-inefficient BH track (Maccarone 2012; Meyer-Hofmeister & Meyer 2014).

In general, NS-LMXBs show weaker radio jets (Migliari & Fender 2006) than BH-LMXBs, with flux densities ranging from hundreds of μJy (for typical distances of ~ 5 kpc) down to only tens of μJy, pushing the observational capabilities of even the most sensitive radio interferometers. Consequently, the connection between X-ray and radio emission in NS-LMXBs remains relatively poorly studied compared to BH-LMXBs (Migliari & Fender 2006, Fender & Muñoz-Darias 2016).

For NS-LMXBs the radio/X-ray luminosity correlation has been well monitored for only three sources so far, showing a wide range of powerlaw indices (4U1728−34: $\beta = 1.4 \pm 0.2$ Migliari et al. 2003; Aql X-1: $\beta = 0.76 \pm 0.1$ and EXO 1745−248: $\beta = 1.7 \pm 0.1$; Tetarenko et al. 2016). However, caution should be taken when interpreting these differences because in some cases the fits are based on a narrow luminosity range (∼ 1 dex). For the complete sample of all Atoll-type NS-LMXBs (those which have been observed simultaneously in the X-ray and radio), an overall correlation was found, showing an index of $\beta \sim 1.4$ (Migliari & Fender 2006), however again the luminosity range studied is also limited. This steep slope implies that NS-LMXB accretion is radiatively efficient (see cyan dashed line in Fig.1), consistent with the idea that accreting material falling onto the surface of the neutron star naturally produces radiation. In fact, NS-LMXBs in the hard state appear to follow a similar radiatively efficient track to the 'outlier' BH-LMXBs, in which the origin of the radiatively-efficient accretion is still not well-established.

In addition to the L_R/L_X hard state correlation, BH-LMXBs show radio flaring before, or at the time of, the transition from the hard to the soft state, preceded by the quenching of the compact jet (Fender et al. 1999, Fender et al. 2009, Gallo et al. 2003, Miller-Jones et al. 2012). For most BH-LMXBs no radio emission has been observed in the soft X-ray state. However, in a few sources there have been some detections of faint radio emission with an inverted spectrum, most likely originating from optically-thin residual jet emission (Fender et al. 2009). At a similar X-ray luminosity, hard and soft-state radio emission can differ in brightness by approximately three orders of magnitude (e.g. by $> 700\times$ for H1743−322; Coriat et al. 2011).

In NS-LMXBs the jet quenching phenomenon is the topic of considerable debate (Fender & Muñoz-Darias 2016;

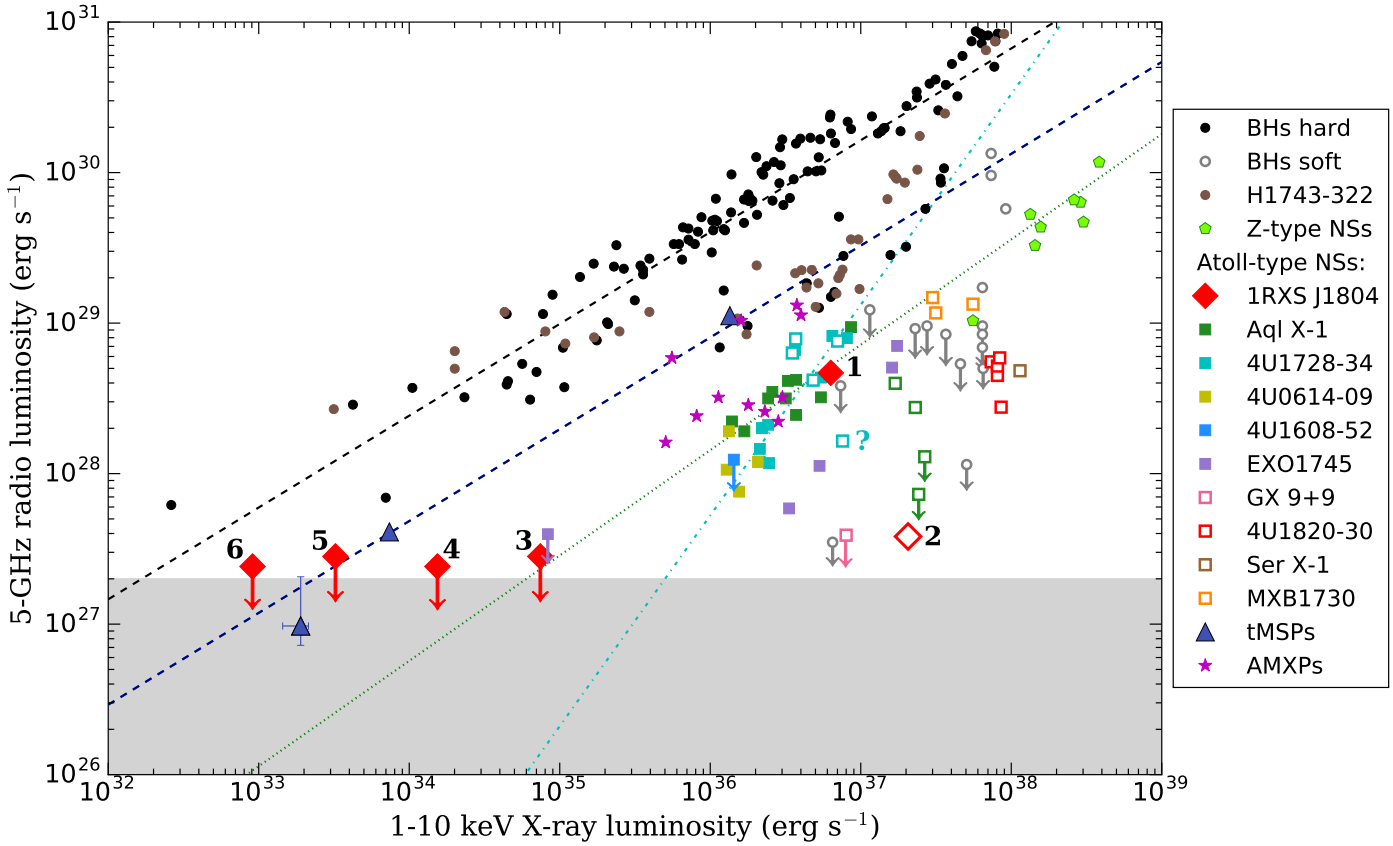


Figure 1. X-ray ($1-10$ keV) luminosity versus radio (5 GHz) luminosity for BH- and NS-LMXBs. The grey shaded area indicates the region of the parameter space that is effectively inaccessible given the sensitivity of current radio telescopes (15 μJy for ~ 1 h integration time) for sources at a typical distance of ~ 5 kpc (note that tMSP PSR J1023+0038, the lowest triangle, is exceptionally close at only 1.3 kpc, which is why it is the only system detected in this region). Circles represent BH-LMXBs; pentagons represent Z-type NS-LMXBs, squares represent Atoll-type NS-LMXBs, and for these we give individual names. Triangles represent tMSPs and stars represent AMXPs. J1804 is represented by red diamonds. Filled symbols represent hard X-ray state observations; open symbols represent soft state X-ray observations. For the single cyan point marked with '?', it is unclear whether this observation was truly in the soft state. The black dashed line represents the radiatively inefficient $L_R \propto L_X^{\beta}$ track of BH-LMXBs, with $\beta \approx 0.6$. The dark blue dashed line represents the tentative $\beta \approx 0.6$ tMSP track proposed by Deller et al. (2015a). The dark green dotted line represents the $\beta \approx 0.7$ track derived for Aql X-1 by Tudose et al. (2009) and Miller-Jones et al. (2010). The cyan dash-dotted line represents the $\beta \approx 1.4$ track derived for 4U1728−34 by Migliari et al. (2003). Data points are taken from: Coriat et al. (2012) for BHs in the hard X-ray state; Coriat et al. (2011) for H1743−322 and most of the BHs in the soft X-ray state; Gierliński et al. (2001) and Russell et al. (2011) for the two lowest upper limits of BHs in the soft state; Migliari & Fender (2006) for Z-type NSs; Tudose et al. (2009) and Miller-Jones et al. (2010) for Aql X-1; Migliari et al. (2003) for 4U1728−34; Migliari et al. (2004) for 4U1820−30 and Ser X-1; Moore et al. (2000) and Kuulkers et al. (2003) for MXB 1730−335; Migliari (2011) for GX 9+9; Tetarenko et al. (2016) for EXO 1745−248; Deller et al. (2015a), Hill et al. (2011) and Papitto et al. (2013) for tMSPs; Migliari et al. (2005) for 4U1608−52, 4U0614−09 and the AMXPs.

Migliari 2011). To date, only two NS-LMXBs have been observed simultaneously in the X-ray and radio bands during both hard and soft X-ray states: 4U1728−34 (Migliari et al. 2003) and Aql X-1 (Tudose et al. 2009, Miller-Jones et al. 2010). For 4U1728−34, only marginal evidence for jet quenching was observed, while in Aql X-1 the jet was quenched by at least one order of magnitude. Furthermore, there are four systems which were observed at radio frequencies only while in the soft state: 4U1820−30, Ser X-1; (Migliari et al. 2004), MXB 1730−355; (Rutledge et al. 1998, Kuulkers et al. 2003) and GX 9+9 (Migliari 2011). 4U1820−30, Ser X-1 and MXB 1730−355 showed surprisingly strong radio emission (if the assumed distance is accurate), albeit at a slightly lower radio luminosity than other hard-state NS-LMXBs (see Fig.1), while no radio emission was detected for GX 9+9 (Migliari 2011). It is important to note that in the case of Atoll-type NS-LMXBs there have been many detections in the soft state (6 out of the 9 systems observed in the radio band), while in BH-LMXBs almost all radio observations in the soft state have provided non-detections. Bearing in mind that NS-LMXBs tend to be less radio loud than BH-LMXBs, the observed level of jet quenching in NS-LMXBs seems to be less extreme than in BH-LMXBs (Migliari & Fender 2006).

1.1 1RXS J180408.9−342058

1RXS J180408.9−342058 (hereafter J1804) was classified as a NS-LMXB system on 16 April 2012 when *INTEGRAL* detected a Type I X-ray burst from a previously unclassified

X-ray source (Chenevez et al. 2012). Assuming that the Eddington luminosity was reached during the burst (Kuulkers et al. 2003), the upper-limit to the distance was estimated to be ~ 5.8 kpc (Chenevez et al. 2012). *Swift*/XRT observations on 17 and 30 April 2012 revealed faint X-ray emission ($L_{X,0.5-10\,\mathrm{keV}} \sim 10^{33-34}$ erg/s), consistent with a very low rate ($\sim 10^{-4} L_{\mathrm{Edd}}$) of accretion (Kaur & Heinke 2012). Based on this, the source was classified as a very faint X-ray transient (VFXT; see Wijnands et al. 2006 for classification details).

On 27 January 2015 the *Swift*/BAT hard X-ray monitor ($15-50$ keV; Matsuoka et al. 2009) detected a new, bright outburst from J1804 (Krimm et al. 2015a), which was later confirmed by *MAXI/GSC* ($2-20$ keV; Negoro et al. 2015). Subsequent *Swift*/BAT observations revealed steady, hard X-ray emission, consistent with canonical accreting LMXB outbursts ($L_{X,15-50\mathrm{keV}} \sim 10^{36-38}$ erg/s). During this outburst, J1804 was monitored in a multiwavelength campaign (X-ray: Boissay et al. 2015, Ludlam et al. 2016,Parikh et al. 2017a; optical and IR: Baglio et al. 2016). In April 2015, J1804 transitioned to the soft X-ray state (Degenaar et al. 2015) before returning to quiescence at the beginning of June 2015 (Parikh et al. 2017a).

It has been suggested (e.g. Degenaar et al. 2014 and Heinke et al. 2015) that some VFXTs may be similar in nature to tMSPs. Furthermore, the X-ray spectrum of J1804 in its initial hard state is consistent with a $\Gamma \sim 1$ power law (Krimm et al. 2015b), which is strikingly hard for typical NS-LMXBs (Parikh et al. 2017b) but similar to that displayed by the tMSPs (Tendulkar et al. 2014). The tMSPs have also been found to be surprisingly bright in radio, even at low X-ray luminosities (Deller et al. 2015a).

In order to investigate the X-ray/radio behaviour of J1804, we performed simultaneous observations with *Swift*/XRT and the Karl G. Jansky Very Large Array (VLA) radio interferometer, monitoring the source through its 2015 outburst and transition back to quiescence. Our aim was to track J1804 in the L_R/L_X diagram, comparing it to typical hard state NS-LMXBs, as well as tMSPs and AMXPs.

Baglio et al. (2016) investigated the near-infrared(NIR)/optical/ultraviolet (UV) spectrum of J1804 during its 2015 outburst. On 26 February 2015, during the hard X-ray state, they found a low-frequency excess in the NIR band, indicating the presence of a jet. Their observations on 24 April 2015, when J1804 was in the soft X-ray state, showed that the NIR excess had disappeared, thus indicating a reduction of the jet emission.

Ludlam et al. (2016) observed J1804 with the *NuSTAR* and *XMM-Newton* X-ray satellites during its 2015 hard X-ray state, finding clear evidence for an Fe K_α line and N VII, O VII and O VIII reflection lines. Using a relativistic reflection model they estimated the inclination of the binary to be $i \sim 18^\circ - 29^\circ$ and the inner radius of the disk $R_{in} \leq 22$km. They found no evidence for coherent X-ray pulsations, indicating that J1804 is apparently a non-pulsating NS-LMXB. Using *NuSTAR* and *Chandra* observations, Degenaar et al. (2016) detected the Fe K_α line during the soft state, finding similar values for the inclination and inner radius of the disk: $i \sim 27^\circ - 35^\circ$, $R_{in} \leq 11 - 17$ km.

In this paper we present the data reduction (§2) and the results of the combined radio/X-ray analysis of J1804 (§3), discussing its implications in comparison to other NS-LMXB systems (§4).

2 OBSERVATIONS AND DATA ANALYSIS

We performed quasi-simultaneous observations of J1804, using the *Swift* X-ray telescope and the VLA radio interferometer, during its outburst in March – June 2015. Table 1 provides a log of all observations used in this work.

2.1 Radio Data (VLA)

J1804 was observed with the VLA at 6 epochs (project ID: 15A-455): each at X-band (8–12 GHz) for a total duration of ~ 1 h including calibration scans, with ~ 30 min on source. During the first 2 epochs in March and April 2015 the array was in B configuration (synthesized beam $\sim 1.25''$), and during the last four epochs the array was transitioning to BnA, gradually increasing in resolution up to $\sim 0.6''$. We used J1331+305 and J1407+2807 as flux and polarization calibrators, and we used J1806−3722 as a phase and amplitude calibrator.

The data were reduced using CASA (McMullin et al. 2007) and the EVLA pipeline. We combined all epochs in one measurement set and used the multi-scale/multi-frequency clean method in CASA (Rich et al. 2008) to make a source model of the field. We then used this model to apply self-calibration corrections to each epoch before imaging and extracting the target flux density (or upper limit). We used phase self-calibration with a solution interval of 12 seconds, and amplitude self-calibration with an interval of 10 minutes. The RMS noise of the per-epoch images was $3-4\,\mu$Jy, and the combined image of all epochs reached a root mean square (RMS) noise of $\sim 2\,\mu$Jy.

For the epochs where the source was detected, we performed spectral and time-series analyses. In the first radio observation we split the 8–12 GHz band into 8 spectral bins, each consisting of 4 subbands, where a subband is a 128-MHz chunk of data comprised of 64 x 2-MHz channels. We imaged each subband with the source model obtained from our full-band imaging at this epoch. For our second observation we applied the same technique; however, due to the faintness of the radio source, we split the band into two 2-GHz subbands.

Figure 2 shows the combined (8 – 12 GHz) radio interferometric map of J1804 and its surroundings, where all 6 observation epochs have been stacked together. In all VLA observations J1804 was unresolved within the 1.9×0.65 arcsecond beam. J1804 is located close to the radio galaxy NVSS J180414−342238 (Condon et al. 1998), whose extended lobes are prominently visible in the upper-left side of the radio image (see Figure 2). The combination of all observations allowed us to create the best model of the extended emission close to the source, allowing us to achieve a sensitivity close to the theoretical thermal noise.

2.2 X-rays (*Swift, MAXI*)

Based on the 6 observation epochs obtained with the VLA, we selected 9 quasi-simultaneous *Swift*/XRT observations (Target ID 32436), i.e. each radio observation is framed by

Table 1. The VLA 10-GHz radio detections and upper limits (3 σ) together with the corresponding quasi-simultaneous *Swift* X-ray observations and spectrum.

Date Swift (2015)	MJD Swift (d)	Obs. ID and obs. mode	Unabs. Flux [a] X-ray (10^{-9}erg/cm^2/s)	Photon index	χ^2_ν	dof	Date VLA (2015)	MJD VLA (d)	Flux density [b] radio (μJy)
16 Mar	57097.29	00032436024(WT)	1.618 ± 0.026	1.12 ± 0.02	1.01	523	17 Mar	57098.59	232 ± 4
19 Mar	57100.35	00032436025(WT)	1.507 ± 0.025	1.18 ± 0.02	1.08	503	-	-	
12 Apr	57124.17	00032436032(WT)	$4.959^{+0.076}_{-0.075}$	1.62 ± 0.04	1.06[c]	502	13 Apr	57125.51	19 ± 4
14 Apr	57126.55	00081451001(WT)	$5.252^{+0.052}_{-0.051}$	1.66 ± 0.03	1.01[c]	599	-	-	
1 Jun	57174.65	00032436035(PC)	$4.120^{+0.45}_{-0.43} \times 10^{-2}$	1.95 ± 0.15	1.02	42	1 Jun	57175.39	< 14
2 Jun	57175.58	00033806001(PC)	$1.502^{+0.15}_{-0.14} \times 10^{-2}$	1.99 ± 0.12	1.09	43	2 Jun	57177.35	< 12
7 Jun	57180.26	00033806002(PC)	$4.01^{+2.81}_{-2.14} \times 10^{-4}$	3.17 ± 1.01	0.53	16	7 Jun	57179.37	< 14
9 Jun	57182.63	00032436037(PC)	$2.12^{+7.67}_{-1.66} \times 10^{-4}$	$3.67^{+2.09}_{-2.79}$	0.29	16	-	-	
11 Jun	57184.58	00033806003(PC)	$2.25^{+1.75}_{-1.63} \times 10^{-4}$	$2.56^{+0.99}_{-1.15}$	0.99	13	11 Jun	57184.27	< 12

[a] X-ray flux in 1–10 keV range (90% confidence interval)
[b] Radio flux density at 10 GHz with 1 σ errors.
[c] For 12 Apr and 14 Apr observations we used an additional blackbody spectral component with temperatures of 0.89±0.07 keV and 0.89±0.04 keV respectively.

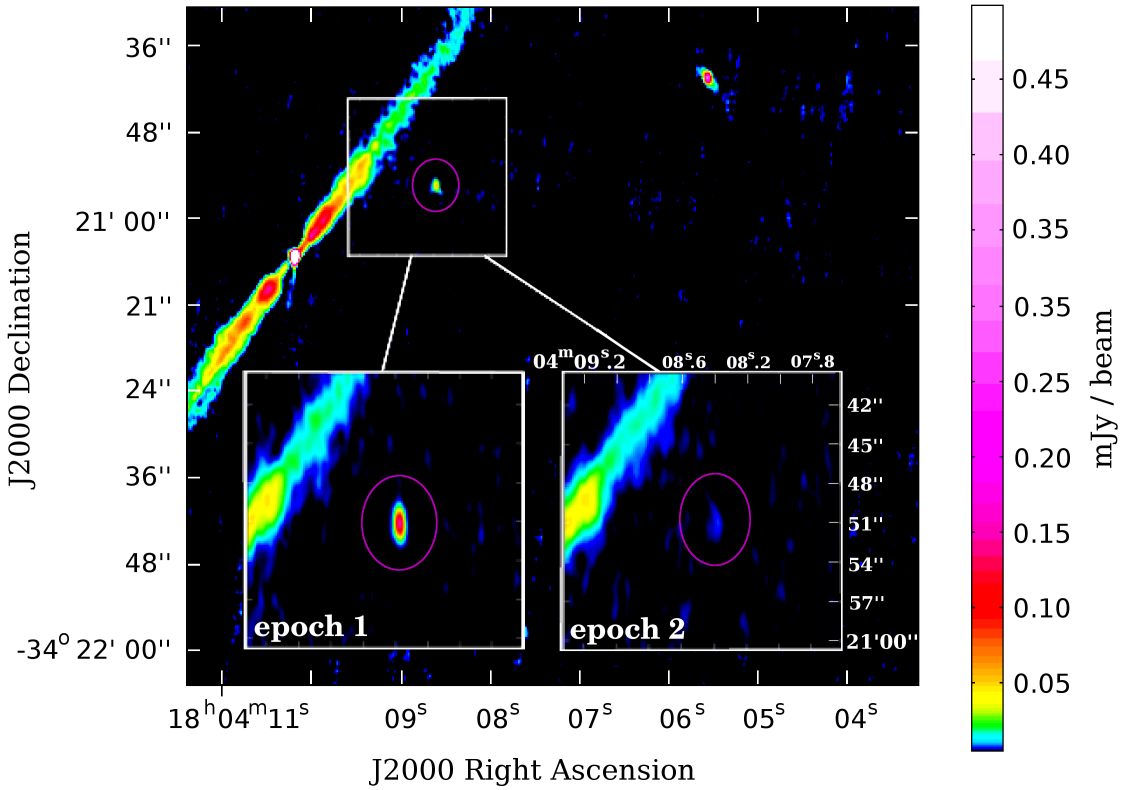


Figure 2. VLA combined radio image (all 6 epochs) of J1804 and the surrounding field. The extended diagonal feature corresponds to the lobes of a nearby radio galaxy (NVSS J180414−342238). The insets at the bottom show images from the first (left) and second (right), epochs individually.

a pair of X-ray observations (for more details see Table 1, Figure 3 and Section 3.3).

In the first 4 observations (March − April 2015), J1804 was bright (unabsorbed $1-10$ keV flux $> 10^{-9}$ erg/cm^2/s) and *Swift* operated in Window Timing (WT) mode with an exposure time per observation of $\sim$ 1 ks. As J1804 returned to quiescence (unabsorbed $1-10$ keV flux $< 10^{-12}$ erg/cm^2/s), the source became faint, such that our final 5 observations were done in Photon Counting (PC) mode with an individual exposure time of ~ 2 ks. For more details about the X-ray light curve see Parikh et al. (2017a).

We used the XRT_PIPELINE task for basic data reduction and calibration. We extracted the spectrum using `xselect`. We used variable in size extraction regions for each

WT epoch, in order to properly correct for *Swift*'s roll angle in these 1-D data sets. For each WT data set, the source and background regions were of equal size. The size of WT-mode event regions was no greater than 30 pixel. In the PC-mode observations we used the same source and background regions (a 30-pixel radius circle area for the source, and a 30-pixel width annulus area for the background with a 30-pixels inner radius). We examined observations that have a count rate more than $150-200$ counts/s in WT-mode and >0.6 counts/s for PC mode in order to check for possible pile-up (following the method in Romano et al. 2006), and excluded the 3 central pixels for the 3rd and 4th observations.

We used the `XRTMKARF` script together with the 'swxwt0to2s6_20131212v015.rmf' response file to produce an ancillary file for each individual observation (using individual exposure maps), correcting for known artifacts on the CCD. The `xselect` tool was used to extract the light curve and flux. We selected photons from the $0.7-10$ keV range for WT mode observations and $0.4-10$ keV for PC mode observations in order to perform the best possible spectral fit with `Xspec`. For the first two observations (in March 2015) an acceptable fit was achieved using an absorbed power law model (`TBabs*powerlaw` in `Xspec`). For the two observations in April 2015, a combination of absorbed power law and black body (`bbody` model in `Xspec` with $\sim$1 keV temperature) models provided a better fit ($\chi^2_\nu \approx 1.0$, dof$\approx$500) than a single power law model ($\chi^2_\nu \approx 1.8$). Parameters of the model and reduced χ^2 value for each epoch are summarized in Table 1. We performed a simultaneous fit for hydrogen column density (nH) value (using `TBabs` model) at all epochs in order to get the best estimate, which was found to be $0.36\pm0.02\times10^{22}$ cm^{-2}. This value is consistent with previous work on this source (e.g. Ludlam et al. 2016, Degenaar et al. 2016). We used `cflux` in `Xspec` to determine unabsorbed $1-10$ keV fluxes and their associated errors for each epoch (see Table 1).

In order to produce a hardness-intensity diagram (HID) for the 2015 outburst of J1804 (see Figure 4), we used publicly available data from *MAXI* ($2-10$ keV)[1] and *Swift*/BAT ($15-50$ keV)[2]. For both bands we converted count rates into Crab flux units assuming a Crab-like spectrum for J1804. We defined hardness ratio as $\mathrm{Flux}_{(15-50\mathrm{keV})}/\mathrm{Flux}_{(2-10\mathrm{keV})}$ and intensity as $\mathrm{Flux}_{(15-50\mathrm{keV})}+\mathrm{Flux}_{(2-10\mathrm{keV})}$.

3 RESULTS

3.1 Radio evolution

J1804 was detected by the VLA in our first two observations. At 10-GHz we measured flux densities of 0.232 ± 0.004 mJy and 0.019 ± 0.004 mJy ($>4\sigma$ detection; see insets of Figure 2), respectively. In the remaining four observations, J1804 was undetected at the best-fit position from observation 1 – with 3-σ flux density upper limits of $\sim0.012-0.014$ mJy. The source was also undetected in a combined image of the last four observations, or any combination of these observations.

We investigated the first and second radio observations (when the source was detected) for variability and spectral shape. In the first epoch no significant variability on a $\sim$1 hour time scale was observed. We also observed no frequency dependence and the 8 – 12 GHz radio spectrum was consistent with being flat, with a powerlaw index of $\alpha=0.12\pm0.18$ (where $S_\nu\propto\nu^\alpha$) in the first observation. During the second radio observation, J1804 was too faint to establish if it was variable over the 1-hour observation timescale. Also, the radio spectrum was not constrained in a meaningful way ($\alpha=-0.31\pm0.68$), such that we could not distinguish between a flat or steep radio spectrum, and we could not identify whether the radio emission was optically-thick or optically-thin.

Using the B-configuration VLA beam size (1.9×0.65 arcsecond) and assuming a distance of 5.8 kpc, we estimate an upper limit of $<7\times10^3$ AU (3×10^6 light-seconds) for the projected linear size of the radio source. Assuming the brightness temperature does not exceed 10^{12} K (see Migliari & Fender 2006), we also estimate a lower size limit of >0.01 AU (5.2 light-seconds) for the first epoch and >0.003 AU (1.48 light-seconds) for the second epoch. Using a $\sim$ 3h orbital period (tentatively proposed by Degenaar et al. 2016) and assuming a total system mass of 2 $M_\odot$ (1.4 $M_\odot$ neutron star and 0.6 $M_\odot$ companion), we determine the J1804 binary would have a semi-major axis of 0.006 AU or $\sim$ 3 light-seconds. In this scenario, the radio emitting region during the first epoch would be larger than the binary separation and the jet would be gravitationally unbound from the system.

Assuming a flat radio spectrum and 5.8-kpc distance we calculate the 5-GHz luminosity[3] of J1804 and compare it to a large sample of BH- and NS-LMXBs (Figure 1).

3.2 Source Position

The radio detection in the first epoch provides the most precise position of J1804 to date:

RA: $18^{\mathrm{h}}04^{\mathrm{m}}08^{\mathrm{s}}.3747\pm0^{\mathrm{s}}.0002$,
Dec: $-34^\circ20'51''.18\pm0''.01$.

Here the fit errors represent the beam size (for the given VLA configuration) divided by signal to noise ratio. These do not account for the uncertainty in the absolute positional accuracy of the phase-referenced VLA observations. However, the reference source J1806−3722 is accurate to $\sim$ 1 mas (defined at 8 GHz), and is only a few degrees from J1804, meaning that any systematic offset in the absolute positions are at worst comparable to the positional errors derived from the VLA beam. This position is about three orders of magnitude more precise than the previous best position provided by optical (Baglio et al. 2015) and ultraviolet (Krimm et al. 2015b) observations and consistent with the position provided by Deller et al. (2015b).

[1] http://maxi.riken.jp/top/index.php?cid=1&jname=J1804-343
[2] http://swift.gsfc.nasa.gov/results/transients/weak/1RXSJ180408.9-342058/

[3] $L_R=4\pi d^2\nu S_\nu$, where d is distance, ν=5 GHz is the reference frequency and S_ν is the flux density at the reference frequency.

3.3 *Swift*

J1804 was detected in all 9 *Swift* observations which we used in our study (Table 1). As can be seen from the full X-ray light curve (see Fig. 3 and Parikh et al. 2017a for more details), the 2015 outburst of J1804 lasted ~ 5 months. The source was in the hard X-ray state until 2015 March, with a typical $(0.5-10\,\mathrm{keV})$ flux of 1.5×10^{-9} erg cm^{-2}s^{-1}, before transitioning to the soft state around 3 April (Degenaar et al. 2015) with a typical flux of $\sim 4\times10^{-9}$ erg cm^{-2}s^{-1} (see photon indices in Table 1 and HID in Figure 4). Several weeks later (around June 6) the flux rapidly decreased as the source returned to its quiescent level ($\sim 10^{-12}$–10^{-13} erg cm^{-2}s^{-1}; Parikh et al. 2017a).

In order to investigate the X-ray/radio correlation, we estimated the X-ray flux values corresponding to the exact times of our radio observations by logarithmically interpolating between six pairs of closely spaced consecutive X-ray observations (see blue circles in Figure 3). In observation 1 we found J1804 right among other NSs in the L_R/L_X diagram. In observation 2 we found the radio emission to be strongly suppressed, providing the lowest soft-state radio detection to date. In observations 3–6 the source was not detected, which rules out that it is as radio bright as tMSPs or AMXPs at low X-ray luminosities.

4 DISCUSSION

4.1 Jet quenching

Jet quenching is a well-established phenomenon in BH-LMXBs. For most BH-LMXBs, quenching of the radio emission is observed immediately before the transition to the soft X-ray state (e.g. Fender et al. 2009). Only a few detections of very faint, optically thin radio emission have been made in the soft state, immediately following hard-to-soft X-ray state transitions (e.g. Coriat et al. 2011). Further into the soft-state (between 5 to 30 days after the transition) and at lower X-ray luminosity, numerous instances of radio non-detections indicate that the soft X-ray state radio jet is heavily suppressed (Hjellming et al. 1999, McClintock et al. 2009, Gallo et al. 2004).

There are only three BH systems (XTE J1650−500; Corbel et al. 2004, GX 339−4; Fender et al. 2009 and XTE J1748−288; Brocksopp et al. 2007) which have been detected in the full soft state (up to a month after the state transition). However, the observed radio emission in these cases was optically thin and (in some cases) the observed behaviour of spatially resolved components indicates that this emission is most likely not from a compact jet, but rather from its remnant: i.e. the interaction of ejected radio blobs with the surrounding interstellar medium or pre-existing jet material (Fender & Muñoz-Darias 2016). For most BH-LMXBs, radio emission is strongly quenched in the soft state and reappears only after the system has transitioned back to the hard state – the most striking example being H1743−322, where the level of quenching was detected to be a factor of more than 700 (Coriat et al. 2011). Soft-state jet quenching (by a factor of $\gtrsim$25) was also observed in Swift J1753.5−0127 (Rushton et al. 2016). Furthermore, LMC X-1 (Gierliński et al. 2001) and 4U1957+11 (Russell et al. 2011), which remain in a persistent soft state, do not show detectable radio emission. This is consistent with the idea that a jet can not be produced in the soft X-ray state and the emission that has been observed in other BH systems in this state could be just a remnant of the transient ejecta.

The physical origin of this quenching is unknown since no widely accepted model of jet production has been developed to date. It is thought that jet production can be further understood by considering how the jet behaves during the different modes of accretion (i.e. X-ray states). The most typical models (see e.g. Meier 2001) suggest that large-scale-height poloidal magnetic fields are responsible for jet production. Indeed, in the hard X-ray state these fields can be provided by a vertically extended accretion flow (i.e. the corona; see Section 1), while at higher accretion rates, in the soft state, a geometrically-thin accretion disk alone cannot provide such a magnetic field and thus cannot sustain a jet (Meier 2001).

Whether jet quenching also occurs in NS-LMXBs is currently unclear. The handful of observed systems show markedly different behaviours.

4U1728−34

4U1728−34 was the first Atoll-type NS-LMXB that was well sampled in the X-ray/radio plane (Migliari et al. 2003). This is a persistent source that was monitored with two separate quasi-simultaneous X-ray/radio campaigns in 2000 and 2001. During the 2000 campaign, 4U1728−34 stayed mostly in the hard X-ray state with two short excursions into the soft state. The radio luminosities in the hard and soft states were almost identical, indicating no radio quenching. One observation (point 'g' in Migliari et al. 2003 Fig.1, or point 'Q2' in Tudose et al. 2009 Fig.9) did provide a lower radio luminosity than other epochs, however, its X-ray state was unclear (see '?' symbol in Figure 1). Therefore, jet quenching cannot be definitively connected to an X-ray state in this case. During the second observational campaign (2001), 4U1728−34 remained in the hard X-ray state with lower X-ray and radio luminosities than observed in the previous campaign (when the system was transitioning between hard and soft X-ray states). Combined observations from both campaigns, mixing hard and soft states, revealed a $\beta = 1.4$ power-law correlation between the observed radio and X-ray luminosities.

Aql X-1

Aql X-1 is one of the best studied NS-LMXBs, going into outburst almost every year. It was found to have a tentative $\beta = 0.7$ power-law correlation between L_R and L_X for hard state observations (Tudose et al. 2009; Tetarenko et al. 2016; see green squares and green dotted line in Figure 1). There were also several radio observations of this source in its soft X-ray state: an upper limit in 2002, a detection in 2004, and an upper limit and detection in 2009 (Miller-Jones et al. 2010; note that the upper limits were significantly deeper than the detections). All observations that have been taken during the soft state appear to be at a lower (up to a factor of 13) radio luminosity for a given L_X than detections obtained during the hard state. Thus, Aql X-1 was the only NS-LMXB that showed a certain degree of jet quenching in the soft X-ray state and at high X-ray luminosity (Miller-Jones et al. 2010). It should be noted that comparing hard and soft radio flux densities from different outbursts of the same source can in some cases be dangerous because NS-

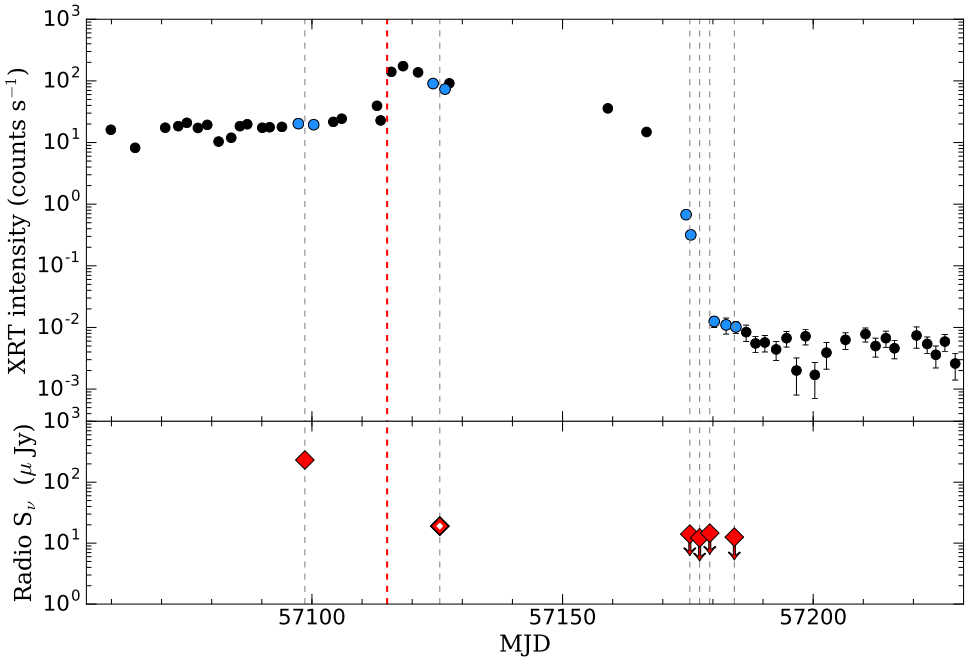


Figure 3. *Top*: *Swift*/XRT ($0.5-10$ keV) X-ray lightcurve of the 2015 outburst of J1804 (data from Parikh et al. 2017a). *Bottom*: VLA (10 GHz) radio lightcurve (S_ν is radio flux density). For each radio observation we selected the two closest X-ray observations in time (blue circles) and reanalyzed those data (Table 1). The grey dashed vertical lines correspond to the MJDs of the radio observations. The red dashed line corresponds to the approximate time of the hard-to-soft X-ray state transition.

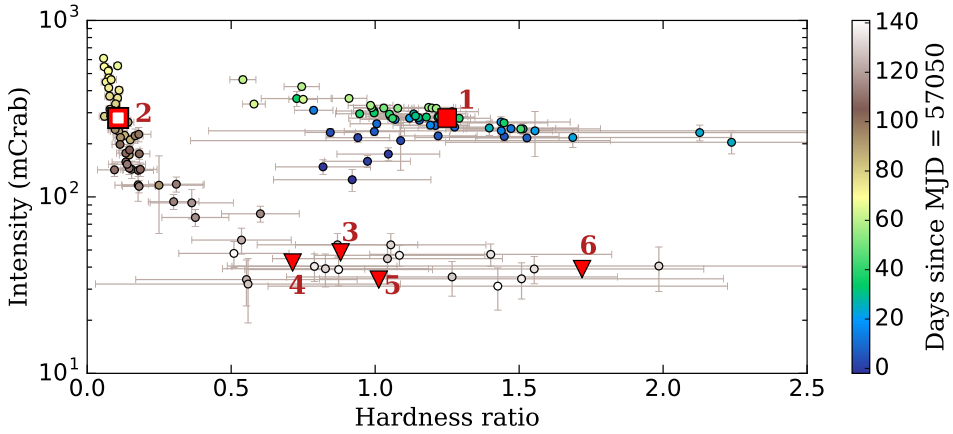


Figure 4. Hardness-intensity diagram of the 2015 outburst of J1804. Red squares represent VLA radio detections, downwards triangles represent radio upper limits. Filled/open symbols indicate radio detections in the hard/soft X-ray state. Circles represent X-ray, *Swift*/BAT and *MAXI* observations, with 1 σ errorbars. The colour scale indicates the number of days since the start of the 2015 outburst. Hardness ratio defined as $\mathrm{Flux}_{(15-50\mathrm{keV})}/\mathrm{Flux}_{(2-10\mathrm{keV})}$ and intensity as $\mathrm{Flux}_{(15-50\mathrm{keV})} + \mathrm{Flux}_{(2-10\mathrm{keV})}$.

LMXBs can have very different hardness-intensity tracks in each outburst (see e.g. Muñoz-Darias et al. 2014). However, over the outbursts in which the radio/X-ray correlation of Aql X-1 was compared, the observed HID tracks appeared very similar (see Tudose et al. 2009, Miller-Jones et al. 2010).

Soft state only NS-LMXBs

NS-LMXBs that have only been observed in the radio during a persistent soft state appear to exhibit two distinct behaviours: a given source is either deeply quenched or shows sustained radio emission. A single observation of GX 9+9 (Migliari 2011) provided a deep radio upper limit ($L_R \lesssim 4 \times 10^{27}$erg/s), indicating strong radio quenching ($\geq$2 orders of magnitude when compared to typical hard state systems at similar X-ray luminosity), similar to soft state BH systems. Ser X-1 and 4U1820−30, which are persistently in outburst (Migliari et al. 2004), appear to show low levels of jet quenching (being detected in radio at a slightly lower level). The few contemporaneous radio and X-

ray observations of these systems revealed around an order of magnitude lower radio emission than what is expected for hard-state NSs by extrapolating the L_R/L_X correlation to higher L_X (Migliari & Fender 2006). However, X-ray monitoring has shown that these systems have transitioned between the hard and soft states, therefore, it is possible that the observed radio emission could be residual emission from a pre-existing hard-state jet. Alternatively, the rapid burster MXB1730−335 (Moore et al. 2000) did not appear to show any jet quenching during its soft X-ray outburst[4]. However, hard-state radio emission has not been observed in any of these three systems and their perceived level of jet quenching has been assumed by comparing their soft-state radio emission to the assumed $\beta = 1.4$ relation for typical hard-state systems. Therefore, we can not determine their true level of jet quenching as reliably as observing hard-to-soft state transitions during the same outburst.

1RXS J180408.9−342058

Observations during both hard and soft X-ray states for a single outburst of the same source are critical to accurately track the evolution of the radio jet and to measure its quenching. So far this has only been achieved for Aql X-1, which showed good evidence for jet quenching (Miller-Jones et al. 2010). Thus, J1804 is only the second source in which we can examine NS-LMXB jet quenching in reasonable detail.

We performed radio observations of J1804 during outburst and its evolution back to quiescence (see HID in Figure 4). During the outburst, the source was detected at radio wavelengths in both hard and soft X-ray states (see Figure 3). We detected J1804 in the rising hard state, finding that its radio and X-ray luminosities were consistent with typical Atoll-type NS-LMXB hard state luminosities. We also significantly detected J1804 in the soft X-ray state. This detection is a factor of $\sim$ 12 lower in flux density than the hard state detection ($\sim$1 month earlier), hence we can firmly claim the occurrence of radio jet quenching by more than an order of magnitude.

The radio spectrum in our first observational epoch was consistent with being flat ($\alpha = 0.12 \pm 0.18$), suggesting optically-thick synchrotron emission from a compact jet. During the soft X-ray state, the radio source was faint ($\sim 19 \pm 4\,\mu$Jy; $\sim 5\sigma$ detection), which precludes any detailed spectral analysis for this observation. The obtained spectral index for this epoch ($\alpha = -0.31 \pm 0.68$) has a large uncertainty and thus does not discriminate between optically thick and optically thin synchrotron emission from a radio jet ($\alpha \approx 0$). This detection is at a lower radio luminosity than any other detected NS-LMXB in outburst[5]. Although GX 9+9 has a similar radio luminosity, this is only an upper limit (see Migliari 2011).

Since we only have one radio observation during the hard state, and one during the soft state (with $\sim$ 1 month separation), it could be argued that the soft-state detection represents residual emission of the hard-state jet (although it is 10 days after the hard-to-soft state transition). Therefore, the true level of quenching could, in principle, be deeper. Remnant radio emission has been seen in BH systems during the soft state (see e.g. Fender et al. 2009 and references therein). In this case, the collimated jet is usually quenched prior to the X-ray state transition and a transient jet is launched during the transition. Therefore, we can not rule out the possibility that both of these events occurred between our first and second radio observations of J1804 and that the observed radio emission in the soft state is residual emission from a transient jet. If this was the case, our soft state detection would be at least a lower limit on the true level of the jet quenching.

NS-LMXBs have shown a broad diversity of behaviour, and only with observations of more such systems, over the widest possible range of radio and X-ray luminosities, can we hope to ascertain whether they show a consistent set of behaviours and make detailed comparisons to BH-LMXBs. Some NS-LMXBs appear to quench in the soft state (e.g. Aql X-1, GX 9+9 and J1804) and others apparently do not (4U1748−34, Ser X-1, 4U1820−30 and MXB1730−335). Therefore, there may exist some tunable parameter that affects jet production and quenching, such as magnetic field strength, spin of the NS and/or mass accretion rate. Migliari 2011 summarised observations of all NS-LMXBs observed in the radio band to determine a unified scheme of jet production based on such parameters, however, they could not identify any evidence for a single parameter being responsible.

Our soft-state radio detection was only possible due to the recent upgrade to the VLA (Perley et al. 2011), which increased its sensitivity by a factor of $\sim$ 10 for similar observations to those here. This increased sensitivity opens up the possibility to study very faint radio sources such as those associated with jet emission in NS-LMXBs. Further increased sensitivity would allow us to study the spectral properties of the radio emission from NS-LMXBs in detail (e.g. distinguishing between optically thin and thick emission) and possibly detect even deeper radio quenching.

4.2 Radio/X-ray correlation

We observed J1804 in the radio during its 2015 outburst, at high X-ray luminosity $L_X > 10^{36}$ erg/s in both hard and soft X-ray states, and at lower X-ray luminosity as it returned towards quiescence (see Figure 1). The source was not detected below $L_X < 10^{35}$ erg/s. Combining a hard-state detection with our quiescent limits, we conclude that J1804 follows a L_R/L_X track with an index of $\beta \gtrsim 0.7$, in agreement with typical non-pulsating NS-LMXBs[6], for which $\beta \approx 1.4$ (Tetarenko et al. 2016).

[4] We analysed publicly available *RXTE* data from 6 and 11 November 1996 (when the radio obervations of Moore et al. (2000) were taken). We found strong blackbody (with temperature $\sim 1 - 3$ keV) and very steep powerlaw ($\Gamma > 3$) components in both spectra. This confirms that radio observations of MXB1730−335 were taken while it was indeed in the soft X-ray state.

[5] Note that one observation of the tMSP PSR J1023+0038 (the lowest triangle point) has a lower radio luminosity (Deller et al. 2015a), owing to its close proximity ($\sim$1 kpc). Likewise, the next tMSP triangle point to the right in Figure 1, which is XSS J12270−4859 (Hill et al. 2011)

[6] Here we make a distinction between pulsating NS-LMXBs, which show coherent X-ray pulsations tied to the NS rotation rate, and non-pulsating NS-LMXBs, which do not

Pulsating NS-LMXBs, such as AMXPs and tMSPs, appear to be more radio bright at low X-ray luminosity ($L_X \sim 10^{32-35}$ erg/s) than non-pulsating systems (see magenta stars and dark blue triangles in Figure 1, $L_X \sim 10^{32-35}$ erg/s range). However, at higher X-ray luminosities ($L_X > 10^{36}$ erg/s), some AMXPs show similar (e.g. radio observations of SAX J1808.4−3658; Rupen et al. 2002, Migliari & Fender 2006) or even lower radio luminosity (see Tudor et al. 2017) compared with non-pulsating systems (assuming that the relative distances are correct). Furthermore, there are three confirmed tMSP systems observed so far: PSR J1023+0038 (Stappers et al. 2014) and XSS J12270−4859 (Bassa et al. 2014) have so far remained in a very low and steady accretion state, and IGR J18245−2452 (M28I; Papitto et al. 2013) also went into full outburst. As suggested by Deller et al. 2015a, these systems possibly obey their own radio/X-ray correlation with $\beta \approx 0.6$ (see the dark blue dashed line in Figure 1). This was suggested by connecting the highest point (M28I) with the two low-accretion-rate systems whose radio brightness is markedly higher than what is expected for non-pulsating NS-LMXBs based on a $\beta = 1.4$ power law correlation.

This difference opens up the possibility to distinguish between different classes of accreting NSs using their radio/X-ray behaviour. However, due to the expectation that they would be too faint to detect, very few NS-LMXBs have been targeted in the radio at low X-ray luminosities ($L_X \sim 10^{32} - 10^{35}$ erg/s). One of the few exceptions is the recent non-detection of EXO 1745−248 (Tetarenko et al. 2016) at an X-ray luminosity of $\sim 10^{35}$ erg/s, which indicates that this system is significantly radio fainter compared with the tMSPs. Lastly, the upper limits provided by J1804 also indicate that the radio emission of some NS-LMXBs at low X-ray luminosity is much less (by at least a factor of a few and possibly by an order of magnitude or more) than that of tMSPs and AMXPs (Deller et al. 2015a, Tudor et al. 2017).

5 CONCLUSION

We find significant radio jet quenching in the non-pulsating NS-LMXB J1804 (by a factor of ∼12) during its transition from hard to soft X-ray states in its 2015 outburst. Such jet quenching has been previously observed, arguably, only in two other NS-LMXBs: Aql X-1, where quasi-simultaneous radio/X-ray data tracked both the hard and soft X-ray states during two outbursts and GX 9+9, where a single upper limit in the soft state is the only available evidence. Other NS-LMXBs studied quasi-simultaneously in radio/X-ray have not clearly shown jet quenching. Furthermore, our radio observations of J1804 at $L_X \sim 10^{35}$ erg/s seem to indicate that it has a lower radio luminosity than previously observed pulsating NS-LMXBs, i.e. the tMSPs and AMXPs. Such behaviour has also been observed in the non-pulsating NS-LMXB EXO 1745−245, which likewise shows only a radio upper-limit at $L_X \sim 10^{35}$ erg/s.

Our results indicate that NS-LMXBs have fundamentally different accretion characteristics within the class. However, only a few systems have been observed in a broad X-ray/radio luminosity range and during various X-ray states. Observations of more systems at $L_X < 10^{36}$ erg/s are needed to characterize this phenomenon.

ACKNOWLEDGEMENTS

NVG acknowledges funding from NOVA. ATD is the recipient of an Australian Research Council Future Fellowship (FT150100415). JWTH acknowledges funding from an NWO Vidi fellowship and from the European Research Council under the European Union's Seventh Framework Programme (FP/2007-2013) / ERC Starting Grant agreement nr. 337062 ("DRAGNET"). JCAMJ is the recipient of an Australian Research Council Future Fellowship (FT140101082). ND is supported by a Vidi grant from NWO and a Marie Curie fellowship (FP-PEOPLE-2013-IEF-627148) from the European Commission. RW and ASP are supported by a NWO Top Grant, Module 1, awarded to RW. TDR acknowledges support from the Netherlands Organisation for Scientific Research (NWO) Veni Fellowship, grant number 639.041.646. DA acknowledges support from the Royal Society. We are grateful to Neil Gehrels and the duty scientists for rapid scheduling of the *Swift* observations. We acknowledge the use of the *Swift* public data archive.

REFERENCES

Baglio M. C., Campana S., D'Avanzo P., 2015, The Astronomer's Telegram, 7100
Baglio M. C., D'Avanzo P., Campana S., Goldoni P., Masetti N., Muñoz-Darias T., Patiño-Álvarez V., Chavushyan V., 2016, A&A, 587, A102
Bassa C. G., et al., 2014, MNRAS, 441, 1825
Begelman M. C., McKee C. F., Shields G. A., 1983, ApJ, 271, 70
Bogdanov S., et al., 2015, ApJ, 806, 148
Boissay R., et al., 2015, The Astronomer's Telegram, 7096
Brocksopp C., Miller-Jones J. C. A., Fender R. P., Stappers B. W., 2007, MNRAS, 378, 1111
Chenevez J., et al., 2012, The Astronomer's Telegram, 4050
Condon J. J., Cotton W. D., Greisen E. W., Yin Q. F., Perley R. A., Taylor G. B., Broderick J. J., 1998, AJ, 115, 1693
Corbel S., Fender R. P., Tzioumis A. K., Nowak M., McIntyre V., Durouchoux P., Sood R., 2000, A&A, 359, 251
Corbel S., Fender R. P., Tomsick J. A., Tzioumis A. K., Tingay S., 2004, ApJ, 617, 1272
Coriat M., et al., 2011, MNRAS, 414, 677
Coriat M., Fender R. P., Dubus G., 2012, MNRAS, 424, 1991
Degenaar N., et al., 2014, ApJ, 792, 109
Degenaar N., et al., 2015, The Astronomer's Telegram, 7352
Degenaar N., et al., 2016, MNRAS, 461, 4049
Deller A. T., et al., 2015a, ApJ, 809, 13
Deller A., et al., 2015b, The Astronomer's Telegram, 7255
Esin A. A., McClintock J. E., Narayan R., 1997, ApJ, 489, 865
Falcke H., Körding E., Markoff S., 2004, A&A, 414, 895
Fender R. P., Kuulkers E., 2001, MNRAS, 324, 923
Fender R., Muñoz-Darias T., 2016, in Haardt F., Gorini V., Moschella U., Treves A., Colpi M., eds, Lecture Notes in Physics, Berlin Springer Verlag Vol. 905, Lecture Notes in Physics, Berlin Springer Verlag. p. 65 (arXiv:1505.03526), doi:10.1007/978-3-319-19416-5_3
Fender R., et al., 1999, ApJ, 519, L165
Fender R. P., Gallo E., Jonker P. G., 2003, MNRAS, 343, L99
Fender R. P., Belloni T. M., Gallo E., 2004a, MNRAS, 355, 1105
Fender R. P., Belloni T. M., Gallo E., 2004b, MNRAS, 355, 1105
Fender R. P., Homan J., Belloni T. M., 2009, MNRAS, 396, 1370

Gallo E., Fender R. P., Pooley G. G., 2003, MNRAS, 344, 60
Gallo E., Corbel S., Fender R. P., Maccarone T. J., Tzioumis A. K., 2004, MNRAS, 347, L52
Gallo E., Fender R. P., Miller-Jones J. C. A., Merloni A., Jonker P. G., Heinz S., Maccarone T. J., van der Klis M., 2006, MNRAS, 370, 1351
Gallo E., Miller B. P., Fender R., 2012, MNRAS, 423, 590
Gallo E., et al., 2014, MNRAS, 445, 290
Gierliński M., Maciołek-Niedźwiecki A., Ebisawa K., 2001, MNRAS, 325, 1253
Hasinger G., van der Klis M., 1989, A&A, 225, 79
Heinke C. O., Bahramian A., Degenaar N., Wijnands R., 2015, MNRAS, 447, 3034
Hill A. B., et al., 2011, MNRAS, 415, 235
Hjellming R. M., et al., 1999, ApJ, 514, 383
Homan J., et al., 2010, ApJ, 719, 201
Homan J., Fridriksson J. K., Wijnands R., Cackett E. M., Degenaar N., Linares M., Lin D., Remillard R. A., 2014, ApJ, 795, 131
Kaur R., Heinke C., 2012, The Astronomer's Telegram, 4085
Krimm H. A., et al., 2015a, The Astronomer's Telegram, 6997
Krimm H. A., Kennea J. A., Siegel M. H., Sbarufatti B., 2015b, The Astronomer's Telegram, 7039
Kuulkers E., den Hartog P. R., in't Zand J. J. M., Verbunt F. W. M., Harris W. E., Cocchi M., 2003, A&A, 399, 663
Ludlam R. M., et al., 2016, ApJ, 824, 37
Maccarone T. J., 2012, preprint, (arXiv:1204.3154)
Malzac J., 2007, Ap&SS, 311, 149
Matsuoka M., et al., 2009, PASJ, 61, 999
McClintock J. E., Remillard R. A., 2006, Black hole binaries. pp 157–213
McClintock J. E., Remillard R. A., Rupen M. P., Torres M. A. P., Steeghs D., Levine A. M., Orosz J. A., 2009, ApJ, 698, 1398
McMullin J. P., Waters B., Schiebel D., Young W., Golap K., 2007, in Shaw R. A., Hill F., Bell D. J., eds, Astronomical Society of the Pacific Conference Series Vol. 376, Astronomical Data Analysis Software and Systems XVI. p. 127
Meier D. L., 2001, ApJ, 548, L9
Merloni A., Heinz S., di Matteo T., 2003, MNRAS, 345, 1057
Meyer-Hofmeister E., Meyer F., 2014, A&A, 562, A142
Migliari S., 2011, in Romero G. E., Sunyaev R. A., Belloni T., eds, IAU Symposium Vol. 275, Jets at All Scales. pp 233–241, doi:10.1017/S174392131001608X
Migliari S., Fender R. P., 2006, MNRAS, 366, 79
Migliari S., Fender R. P., Rupen M., Jonker P. G., Klein-Wolt M., Hjellming R. M., van der Klis M., 2003, MNRAS, 342, L67
Migliari S., Fender R. P., Rupen M., Wachter S., Jonker P. G., Homan J., van der Klis M., 2004, MNRAS, 351, 186
Migliari S., Fender R. P., van der Klis M., 2005, MNRAS, 363, 112
Miller-Jones J. C. A., et al., 2010, ApJ, 716, L109
Miller-Jones J. C. A., et al., 2012, MNRAS, 421, 468
Mirabel I. F., Rodríguez L. F., 1994, Nature, 371, 46
Moore C. B., Rutledge R. E., Fox D. W., Guerriero R. A., Lewin W. H. G., Fender R., van Paradijs J., 2000, ApJ, 532, 1181
Muñoz-Darias T., Fender R. P., Motta S. E., Belloni T. M., 2014, MNRAS, 443, 3270
Narayan R., Yi I., 1995, ApJ, 452, 710
Negoro H., et al., 2015, The Astronomer's Telegram, 7008
Papitto A., et al., 2013, Nature, 501, 517
Parikh A. S., et al., 2017a, MNRAS, 466, 4074
Parikh A. S., Wijnands R., Degenaar N., Altamirano D., Patruno A., Gusinskaia N. V., Hessels J. W. T., 2017b, MNRAS, 468, 3979
Patruno A., Watts A. L., 2012, preprint, (arXiv:1206.2727)
Perley R. A., Chandler C. J., Butler B. J., Wrobel J. M., 2011, ApJ, 739, L1
Plotkin R. M., Markoff S., Kelly B. C., Körding E., Anderson S. F., 2012, MNRAS, 419, 267
Rich J. W., de Blok W. J. G., Cornwell T. J., Brinks E., Walter F., Bagetakos I., Kennicutt Jr. R. C., 2008, AJ, 136, 2897
Romano P., et al., 2006, Nuovo Cimento B Serie, 121, 1067
Rupen M. P., Dhawan V., Mioduszewski A. J., Stappers B. W., Gaensler B. M., 2002, IAU Circ., 7997
Rushton A. P., et al., 2016, MNRAS, 463, 628
Russell D. M., Miller-Jones J. C. A., Maccarone T. J., Yang Y. J., Fender R. P., Lewis F., 2011, ApJ, 739, L19
Rutledge R., Moore C., Fox D., Lewin W., van Paradijs J., 1998, IAU Circ., 6813
Shakura N. I., Sunyaev R. A., 1973, A&A, 24, 337
Stappers B. W., et al., 2014, ApJ, 790, 39
Tendulkar S. P., et al., 2014, ApJ, 791, 77
Tetarenko A. J., et al., 2016, MNRAS, 460, 345
Tudor V., et al., 2017, preprint, (arXiv:1705.05071)
Tudose V., Fender R. P., Linares M., Maitra D., van der Klis M., 2009, MNRAS, 400, 2111
Wijnands R., et al., 2006, A&A, 449, 1117

This paper has been typeset from a TEX/LATEX file prepared by the author.